

# 000 001 002 003 004 005 006 007 008 009 010 011 012 013 014 015 016 017 018 019 020 021 022 023 024 025 026 027 028 029 030 031 HEAPR: HESSIAN-BASED EFFICIENT ATOMIC EXPERT PRUNING IN OUTPUT SPACE

005 **Anonymous authors**

006 Paper under double-blind review

## 009 ABSTRACT

012 Mixture-of-Experts (MoE) architectures in large language models (LLMs) deliver  
013 exceptional performance and reduced inference costs compared to dense LLMs.  
014 However, their large parameter counts result in prohibitive memory requirements,  
015 limiting practical deployment. While existing pruning methods primarily focus  
016 on expert-level pruning, this coarse granularity often leads to substantial accu-  
017 racy degradation. In this work, we introduce HEAPR, a novel pruning algorithm  
018 that decomposes experts into smaller, indivisible atomic experts, enabling more  
019 precise and flexible atomic expert pruning. To measure the importance of each  
020 atomic expert, we leverage second-order information based on principles similar  
021 to Optimal Brain Surgeon (OBS) theory. To address the computational and stor-  
022 age challenges posed by second-order information, HEAPR exploits the inherent  
023 properties of atomic experts to transform the second-order information from ex-  
024 pert parameters into that of atomic expert parameters, and further simplifies it to  
025 the second-order information of atomic expert outputs. This approach reduces the  
026 space complexity from  $\mathcal{O}(d^4)$ , where  $d$  is the model’s dimensionality, to  $\mathcal{O}(d^2)$ .  
027 HEAPR requires only two forward passes and one backward pass on a small cali-  
028 bration set to compute the importance of atomic experts. Extensive experiments on  
029 MoE models, including DeepSeek MoE and Qwen MoE family, demonstrate that  
030 HEAPR outperforms existing expert-level pruning methods across a wide range of  
031 compression ratios and benchmarks. Specifically, HEAPR achieves nearly lossless  
032 compression at compression ratios of 20%  $\sim$  25% in most models, while also re-  
033 ducing FLOPs nearly by 20%. The code can be found at anonymous-code-B927.

## 034 1 INTRODUCTION

037 Mixture-of-experts (MoE) models have recently emerged as a promising alternative to dense large  
038 language models (LLMs), replacing dense feed-forward layers with sparsely activated experts and  
039 dynamic routing. This design allows MoE models to match or surpass the performance of dense  
040 LLMs while activating only a fraction of parameters during inference (Fedus et al., 2022; Zhu et al.,  
041 2024; Liu et al., 2024a), making them particularly attractive for large-scale, concurrent deployment.  
042 However, while sparse activation reduces computational cost, it exacerbates memory requirements.  
043 For example, DeepSeek-V3 (Liu et al., 2024a) activates only 37B parameters per inference, yet all  
044 671B parameters must still be stored in GPU memory, resulting in prohibitively high deployment  
045 costs. Notably, MoE layers typically account for over 97% of total model parameters, and they  
046 represent the dominant storage bottleneck. Therefore, compressing MoE layers becomes critical to  
047 overcoming inference inefficiency and making deployment feasible in resource-constrained devices.

048 Model pruning has been widely explored as an effective compression strategy to reduce stor-  
049 age and improve efficiency. Yet a fundamental trade-off persists: fine-grained pruning typically  
050 preserves accuracy but yields limited speedups on hardware, whereas coarse-grained pruning di-  
051 rectly enables acceleration but often incurs obvious accuracy loss. Within MoE models, pa-  
052 rameter sparsification (Xie et al., 2024) faces similar limitations, as hardware inefficiencies con-  
053 strain its practical benefits. Consequently, recent research has shifted toward expert-level prun-  
054 ing, offering more direct gains in both acceleration and memory reduction. Existing expert-  
055 level approaches at this level can be broadly divided into expert dropping and expert merging.

054 Expert dropping methods (Lu et al., 2024;  
 055 Huang et al., 2025) completely remove ex-  
 056 perts deemed unimportant, but relying solely on  
 057 calibration to discard entire experts risks los-  
 058 ing valuable complementary expertise, conse-  
 059 quently often leading to notable performance  
 060 degradation. Expert merging methods (Li et al.,  
 061 2024; Chen et al., 2025; Huang et al., 2025)  
 062 instead aim to consolidate functionally simi-  
 063 lar experts to more effectively preserve over-  
 064 all model capacity. However, their clustering-  
 065 based similarity measures are notoriously un-  
 066 stable, and naive merging strategies (e.g., aver-  
 067 aging or frequency-based weighting) often in-  
 068 troduce destructive parameter conflicts, result-  
 069 ing in suboptimal and inefficient outcomes. To  
 070 alleviate these critical conflicts, recent decompositon-based approaches (Li et al., 2025c; Gu et al.,  
 071 2025) represent individual experts as a mixture of shared and specialized components. While this  
 072 advanced framework helps to preserve model capacity, it still requires computationally expensive  
 073 decomposition and merging operations, and unfortunately still incurs a non-negligible accuracy loss.

074 To identify pruning units that are more flexible than expert-level pruning, we introduce the concept  
 075 of an atomic expert, in which each expert is decomposed into smaller, indivisible units. Concretely,  
 076 each atomic expert is defined by jointly grouping the relevant columns of  $\mathbf{W}^{\text{up}}$ ,  $\mathbf{W}^{\text{gate}}$ , and the  
 077 corresponding row of  $\mathbf{W}^{\text{down}}$  (as shown in Figure 1). The output of a full expert can be represented  
 078 as the sum of outputs from multiple atomic experts. Pruning at this granularity directly removes  
 079 atomic experts, thereby isolating pruning effects and avoiding interference with remaining compo-  
 080 nents. By eliminating atomic experts that contribute little to final predictions, inference efficiency  
 081 can be improved and deployment overhead reduced in a more straightforward and essential way.

082 The key challenge now lies in how to quantify the importance of each atomic expert to overall per-  
 083 formance. To tackle this problem, we propose HEAPr, a principled framework for efficient and  
 084 high-performance atomic expert pruning. Our approach is inspired by the classical Optimal Brain  
 085 Surgeon (OBS) theory (Hassibi et al., 1993; LeCun et al., 1989), which approximates the effect of  
 086 weight pruning via a Taylor expansion of the loss function and leverages second-order information  
 087 to identify parameters with minimal contribution. However, applying OBS to modern deep archi-  
 088 tectures is computationally prohibitive due to the cost of Hessian estimation, and this is why layer-  
 089 wise Hessian estimation has become widely adopted (Dong et al., 2017; Frantar & Alistarh, 2022;  
 090 Frantar et al., 2023). Despite this, the space complexity of Hessian estimation at the expert level  
 091 remains  $\mathcal{O}((3d_{\text{model}} \cdot d_{\text{inter}})^2)$ <sup>1</sup>, which is still unacceptable. Therefore, we propose two optimiza-  
 092 tions to improve Hessian matrix computation. First, by decomposing experts into atomic experts,  
 093 we demonstrate that the second-order derivatives of parameters between different atomic experts are  
 094 zero. This observation allows us to significantly reduce the space complexity of the Hessian matrix,  
 095 lowering it to  $\mathcal{O}((3d_{\text{model}})^2 \cdot d_{\text{inter}})$ . Second, we further optimize the Hessian matrix by shifting  
 096 the pruning constraints analysis from the parameter space of atomic experts to their output space.  
 097 This shift enables us to leverage the Fisher information matrix, which is theoretically equivalent to  
 098 the expected Hessian but significantly more efficient to compute (Bishop & Nasrabadi, 2006; Singh  
 099 & Alistarh, 2020), and by combining this with a Taylor expansion of the atomic expert function,  
 100 we can accurately estimate each atomic expert’s contribution to the final loss. This further reduces  
 101 the Hessian complexity to  $\mathcal{O}(d_{\text{model}}^2)$  for each expert, ensuring high efficiency in both computation  
 102 and storage. HEAPr is not only tractable but also highly efficient: all atomic expert importance can  
 103 be computed with just two forward passes and one backward pass on a small calibration set. We  
 104 evaluated HEAPr on seven zero-shot tasks, achieving **nearly lossless** compression with 20% pruning  
 105 on DeepSeekMoE-16B-Base, 25% pruning on Qwen1.5-MoE-A2.7B-Chat, and 40% pruning on  
 106 Qwen2-57B-A14B. Additionally, on the latest Qwen3-30B-A3B model, the average accuracy only  
 107 drops by 0.03 at a 25% compression ratio. Overall, our contributions are summarized as follows:

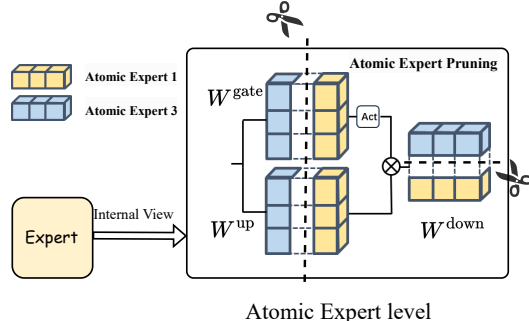


Figure 1: Illustration of atomic expert-level pruning, which removing the  $t$ -th column from the  $\mathbf{W}^{\text{gate}}$  and  $\mathbf{W}^{\text{up}}$  matrices, and the corresponding  $t$ -th row from the  $\mathbf{W}^{\text{down}}$  matrix.

- We introduce a second-order approximation scheme for atomic expert pruning in MoE models, which transforms the second-order information from expert parameters into that

<sup>1</sup> $d_{\text{inter}}$  is the intermediate dimension after the  $\mathbf{W}^{\text{up}}$  transformation, and  $d_{\text{model}}$  is the hidden size of the model.

108 of atomic expert parameters, and further simplifies it to the second-order information of  
 109 atomic expert outputs. This approach reduces the space complexity of second-order infor-  
 110 mation from  $\mathcal{O}((3d_{\text{model}} \cdot d_{\text{inter}})^2)$  to  $\mathcal{O}(d_{\text{model}}^2)$ .  
 111

- 112 • Building on this efficient scheme, we propose HEAPr, a highly efficient and scalable prun-  
 113 ing algorithm that accurately estimates the importance of all atomic experts with just two  
 114 forward passes and one backward pass on a small calibration set.
- 115 • We conduct extensive experiments on DeepSeekMoE-16B-Base, Qwen1.5-MoE-A2.7B-  
 116 Chat, Qwen2-57B-A14B, and Qwen3-30B-A3B across diverse benchmarks. HEAPr out-  
 117 performs current SOTA methods and achieves nearly lossless compression at compression  
 118 ratios of 20%–25% in most models, while also reducing FLOPs by nearly 20%.

## 2 RELATED WORKS AND PRELIMINARY

121 **Mixture of Experts Compression.** Model compression for MoE architectures has recently at-  
 122 tracted growing attention due to the remarkable performance of MoE models. MoE-Pruner (Xie  
 123 et al., 2024) performs weights sparsification based on activation magnitude, weight magnitude, and  
 124 router importance, yet its acceleration is hardware-dependent and relies on distillation to recover  
 125 accuracy. Expert-level pruning has been more extensively explored due to its hardware-friendly  
 126 acceleration. NAEE (Lu et al., 2024) selects a subset of experts to minimize calibration error, but  
 127 this can lead to overfitting and the loss of specialized knowledge. Similarly, MoE-I<sup>2</sup> (Yang et al.,  
 128 2024) combines expert pruning with low-rank decomposition, yet requires additional fine-tuning for  
 129 recovery. To alleviate such issues, expert merging methods aim to retain similar experts rather than  
 130 discarding them. MC-SMoE (Li et al., 2024) merges experts by clustering based on routing poli-  
 131 cies, and HC-MoE (Chen et al., 2025) does so by grouping experts with similar outputs. However,  
 132 limited expert similarity makes merging prone to parameter conflicts. EEP (Liu et al., 2024b) uses  
 133 gradient-free evolutionary search to combine expert dropping and expert merging, cutting SMoE  
 134 experts and active experts while maintaining or improving downstream performance. To further ex-  
 135 ploit redundancy,  $D^2$ -MoE (Gu et al., 2025) constructs a shared expert via weighted combinations  
 136 and compresses residuals through low-rank decomposition, while Sub-MoE (Li et al., 2025a) applies  
 137 SVD to extract a shared subspace across experts, both of which require computationally expensive  
 138 decomposition and merging operations. We decompose the expert into atomic experts and propose  
 139 HEAPr, a method that measures importance by utilizing a second-order approximation to assess the  
 140 importance of atomic experts. This approach enables more flexible pruning units and provides a  
 141 efficient highly [algorithm](#), preserving model performance while eliminating the need for retraining.

142 **Optimal Brain Surgeon in Pruning.** The OBS framework (Hassibi et al., 1993; LeCun et al.,  
 143 1989) approaches pruning as an optimization problem, aiming to minimize the increase in the loss  
 144 function when a parameter is removed. Consider a model that has already been trained and con-  
 145 verged, with parameters  $\theta$  and a corresponding loss  $\ell(\theta)$ . We can analyze the effect of perturbing  
 146 the parameters by analyzing the second-order Taylor expansion of the loss function around  $\theta$ . Specif-  
 147 ically, the change in the loss  $\Delta\ell$  when perturbing the parameters by  $\delta\theta$  is given by the following:

$$\Delta\ell = \ell(\theta + \delta\theta) - \ell(\theta) = \nabla\ell(\theta)^\top \delta\theta + \frac{1}{2} \delta\theta^\top \mathbf{H} \delta\theta + O(\|\delta\theta\|^3), \quad (1)$$

148 where  $\mathbf{H}$  is the Hessian matrix of second derivatives of the loss with respect to the model parameters.  
 149 Since the model has already converged to a local minimum of the loss function, the first-order term  
 150 can be removed ( $\nabla\ell(\theta) = \mathbf{0}$ ), and the higher-order terms can be ignored for small perturbations.

153 For pruning, the constraint is  $\theta_q + \delta\theta_q = 0$  for the target, leading to the optimization problem as:

$$\min_{\delta\theta_q} \frac{1}{2} \delta\theta^\top \mathbf{H} \delta\theta, \quad \text{s.t. } \delta\theta_q + \theta_q = 0, \quad (2)$$

157 where  $q$  denotes the index of the pruned parameter. Solving this optimization problem yields the  
 158 minimal increase in loss from pruning parameter  $\theta_q$ , which is  $\Delta\ell = \frac{1}{2} \frac{\theta_q^2}{[\mathbf{H}^{-1}]_{qq}}$ .

159 Directly computing the full Hessian in deep neural networks is practically infeasible. Existing  
 160 OBS methods to adopt significant approximations. For instance, K-FAC approximation (Martens  
 161 & Grosse, 2015) provides an efficient approximation of second-order information and Hessians are

162 computed layer-wise to guide pruning (Dong et al., 2017; Frantar & Alistarh, 2022; Frantar et al.,  
 163 2023). Previous work (Singh & Alistarh, 2020) shows that the Fisher information matrix serves as a  
 164 reliable Hessian estimate and allows for more efficient computation. Some apply OBS to structured  
 165 pruning (Yu et al., 2022), but these efforts are limited as they consider only the trace of the Hessian.  
 166

### 167 3 METHOD

#### 169 3.1 ATOMIC EXPERT IN MIXTURE-OF-EXPERTS.

171 The MoE architecture has been widely adopted in LLMs as a replacement for the dense feed-forward  
 172 network layer, which effectively increases the model capacity while reducing the number of activated  
 173 parameters. Formally, given an input token representation  $\mathbf{x} \in \mathbb{R}^{d_{\text{model}}}$ , the output of the MoE layer  
 174 with  $N_{\text{exp}}$  experts is defined as:

$$175 \quad \mathbf{y} = \sum_{i=1}^{\kappa} g_i(\mathbf{x}) E_i(\mathbf{x}), \quad \mathbf{g}(\mathbf{x}) = (g_1(\mathbf{x}), \dots, g_{\kappa}(\mathbf{x})) = \text{Top-}\kappa(\mathbf{W}^{\text{gate}} \mathbf{x}) \in \mathbb{R}^{\kappa}, \quad (3)$$

178 where  $\mathbf{W}^{\text{gate}} \in \mathbb{R}^{N_{\text{exp}} \times d_{\text{model}}}$  produces router scores and Top- $\kappa(\cdot)$  denotes the router function that  
 179 selects the top- $\kappa$  experts. Each expert  $E_i(\cdot)$  is a gated feed-forward block:

$$181 \quad E_i(\mathbf{x}) = \mathbf{W}_i^{\text{down}} [\text{SiLU}(\mathbf{W}_i^{\text{gate}} \mathbf{x}) \odot (\mathbf{W}_i^{\text{up}} \mathbf{x})], \quad (4)$$

182 where  $\mathbf{W}_i^{\text{up}}, \mathbf{W}_i^{\text{gate}} \in \mathbb{R}^{d_{\text{inter}} \times d_{\text{model}}}$ ,  $\mathbf{W}_i^{\text{down}} \in \mathbb{R}^{d_{\text{model}} \times d_{\text{inter}}}$ ,  $\odot$  denotes the Hadamard product, and  
 183  $\text{SiLU}(\cdot)$  is the SiLU activation. Within each expert, computations can be decomposed into atomic  
 184 experts. Let  $\mathbf{w}_{i,j}^{\text{up}}$  and  $\mathbf{w}_{i,j}^{\text{gate}}$  denote the  $j$ -th rows of  $\mathbf{W}_i^{\text{up}}$  and  $\mathbf{W}_i^{\text{gate}}$ , respectively, and let  $\mathbf{w}_{i,j}^{\text{down}}$   
 185 denote the  $j$ -th column of  $\mathbf{W}_i^{\text{down}}$ . Then the  $j$ -th atomic expert of the  $i$ -th expert is

$$187 \quad \mathbf{e}_i^{(j)}(\mathbf{x}) = \mathbf{w}_{i,j}^{\text{down}} [\text{SiLU}(\mathbf{w}_{i,j}^{\text{gate}} \mathbf{x}) \cdot (\mathbf{w}_{i,j}^{\text{up}} \mathbf{x})] \in \mathbb{R}^{d_{\text{model}}}, \quad (5)$$

189 where  $\mathbf{w}_{i,j}^{\text{up}}, \mathbf{w}_{i,j}^{\text{gate}} \in \mathbb{R}^{1 \times d_{\text{model}}}$  and  $\mathbf{w}_{i,j}^{\text{down}} \in \mathbb{R}^{d_{\text{model}} \times 1}$ . Consequently, each expert is a linear combi-  
 190 nation of its atomic experts:

$$191 \quad E_i(\mathbf{x}) = \sum_{j=1}^{d_{\text{inter}}} \mathbf{e}_i^{(j)}(\mathbf{x}). \quad (6)$$

194 In this framework, each expert  $E_i(\cdot)$  can be viewed as a linear combination of its atomic experts.  
 195 This decomposition allows pruning at the atomic expert level without compromising the other atomic  
 196 expert structure, leading to both computational acceleration and deployment efficiency directly.

#### 198 3.2 ATOMIC EXPERT IMPORTANCE ANALYSIS IN THE OUTPUT SPACE

200 **Importance of Atomic Experts.** As discussed in Section 2, the OBS theory provides an excellent  
 201 framework for analyzing the impact of parameter pruning on model performance. However, its  
 202 major limitation is the large Hessian matrix, even when only computed layer-wise. In the case  
 203 of MoE, directly applying OBS at the expert level is still infeasible, as it requires constructing an  
 204 exceedingly large Hessian with space complexity of  $\mathcal{O}((3d_{\text{model}} \cdot d_{\text{inter}})^2)$  per expert, leading to  
 205 prohibitive computation and storage costs. Fortunately, by decomposing the expert into smaller  
 206 atomic experts, a property is revealed: the parameters of different atomic experts are decoupled, *i.e.*,

$$207 \quad \frac{\partial^2 E(\mathbf{x})}{\partial \Theta^{(i)} \partial \Theta^{(j)}} = \frac{\partial^2 \mathbf{e}^{(i)}(\mathbf{x})}{\partial \Theta^{(i)} \partial \Theta^{(j)}} = 0, \quad \forall i \neq j \quad (7)$$

209 where  $\Theta^{(i)} \in \mathbb{R}^{3d_{\text{model}}}$  represents the parameters of the  $i$ -th atomic expert. This means that the  
 210 cross-Hessians between different atomic experts are zero, which provides a valuable and simplifying  
 211 property that allows us to focus exclusively on the Hessian of each individual atomic expert with  
 212 respect to its own specific parameters. Based on this observation, the second-order Taylor expansion  
 213 of the change in the loss function with respect to each expert’s parameters can be expressed as:

$$214 \quad \Delta \ell \approx \frac{1}{2} \delta \Theta^T \mathbf{H} \delta \Theta = \frac{1}{2} \sum_{i=1}^{d_{\text{inter}}} (\delta \Theta^{(i)})^T \mathbf{H}^{(i)} \delta \Theta^{(i)} \quad (8)$$

here,  $\Theta \in \mathbb{R}^{3d_{\text{model}} \cdot d_{\text{inter}}}$  denotes the parameters of a given expert, and  $\mathbf{H}$  is the corresponding Hessian matrix with space complexity  $\mathcal{O}((3d_{\text{model}} \cdot d_{\text{inner}})^2)$ . And each  $\mathbf{H}^{(i)}$  represents the Hessian for the  $i$ -th atomic expert. This decomposition leads to a significant reduction in the complexity of summing over the Hessians  $\sum_{i=1}^{d_{\text{inter}}} \mathbf{H}^{(i)}$ , which is reduced to  $\mathcal{O}((3d_{\text{model}})^2 \cdot d_{\text{inter}})$ .

However, the resulting Hessian matrix computation remains unacceptable due to its high computational and storage cost. To further alleviate the bottleneck, we introduce a second optimization that reformulates the pruning constraint. The original parameter-space constraint (equation 2) implies that the atomic expert’s output  $\mathbf{e}_{\mathcal{P}}(\mathbf{x}; \Theta_{\mathcal{P}} + \delta\Theta_{\mathcal{P}})$ , where  $\Theta_{\mathcal{P}} \in \mathbb{R}^{3d_{\text{model}}}$  denotes the parameters of the atomic expert to be pruned, would be zero for every possible input  $\mathbf{x}$ . Although theoretically sound, enforcing such a universal constraint is computationally infeasible. This motivates a more targeted reformulation: for a specific token  $\mathbf{x}$ , what is the minimum loss increase  $\Delta\ell(\mathbf{x})$  required to force the expert’s output to zero? To make this question concrete, we impose the per-token constraint  $\mathbf{e}_{\mathcal{P}}(\mathbf{x}; \Theta_{\mathcal{P}} + \delta\Theta_{\mathcal{P}}) = 0$ , treating  $\mathbf{x}$  as given. Since the atomic expert functions are not optimized with respect to the parameters  $\Theta_{\mathcal{P}}$  through gradient descent, applying a Taylor expansion of the atomic expert functions around  $\Theta_{\mathcal{P}}$  results in the first-order term dominating, yielding:

$$\mathbf{e}_{\mathcal{P}}(\mathbf{x}; \Theta_{\mathcal{P}} + \delta\Theta_{\mathcal{P}}) \approx \mathbf{e}_{\mathcal{P}}(\mathbf{x}; \Theta_{\mathcal{P}}) + \mathbf{J}_{\mathcal{P}}\delta\Theta_{\mathcal{P}} = \mathbf{0}, \quad (9)$$

where  $\mathbf{J}_{\mathcal{P}} \in \mathbb{R}^{d_{\text{model}} \times 3d_{\text{model}}}$  denotes the Jacobian of  $\mathbf{e}_{\mathcal{P}}(\mathbf{x}; \Theta_{\mathcal{P}})$ . This leads to the following problem:

$$\min_{\Theta_{\mathcal{P}}} \frac{1}{2} \sum_{i=1}^{d_{\text{inter}}} (\delta\Theta^{(i)})^T \mathbf{H}^{(i)} \delta\Theta^{(i)} \quad \text{s.t.} \quad \mathbf{J}_{\mathcal{P}} \delta\Theta_{\mathcal{P}} + \mathbf{e}_{\mathcal{P}} = \mathbf{0}. \quad (10)$$

To solve the problem in equation 10, we consider the LLMs trained with a negative log-likelihood loss  $\ell$  (e.g., cross-entropy loss). In this setting, the Fisher Information Matrix  $\mathbf{F}$  is equivalent to the expected Hessian (Bishop & Nasrabadi, 2006), providing a computationally efficient alternative:

$$\mathbb{E}[\mathbf{H}] = \mathbf{F} = \mathbb{E}[(\nabla_{\Theta}\ell)(\nabla_{\Theta}\ell)^T], \quad (11)$$

where  $\ell$  is the sample-wise loss. Previous work (Singh & Alistarh, 2020) has shown that for well-converged neural networks, a few hundred representative samples are already sufficiently reliable to estimate  $\mathbb{E}[\mathbf{H}]$ . Expanding the gradient of  $\ell$  with respect to the parameters gives  $\nabla_{\Theta_{\mathcal{P}}}\ell = \mathbf{J}_{\mathcal{P}}^T \mathbf{g}_{\mathcal{P}}$ , where  $\mathbf{g}_{\mathcal{P}} \in \mathbb{R}^{d_{\text{model}}}$  is the gradient of the loss with respect to the pruned atomic expert output  $\mathbf{e}_{\mathcal{P}}$ . Substituting this expression into the objective equation 10 yields the expected loss increase when pruning the atomic expert  $\mathbf{e}_{\mathcal{P}}$ , with  $\delta\Theta^{(i)} = \mathbf{0}$  for all atomic experts not pruned:

$$\frac{1}{2} \delta\Theta_{\mathcal{P}}^T \mathbb{E}[\mathbf{H}_{\mathcal{P}}] \delta\Theta_{\mathcal{P}} \approx \frac{1}{2} \mathbf{e}_{\mathcal{P}}^T \mathbb{E}[\mathbf{g}_{\mathcal{P}} \mathbf{g}_{\mathcal{P}}^T] \mathbf{e}_{\mathcal{P}}. \quad (12)$$

This leads us to define the **Importance** of the atomic expert  $\mathbf{e}_{\mathcal{P}}$  as

$$s = \mathbb{E}_{\mathbf{x} \sim D} [\Delta\ell] \approx \mathbb{E}_{\mathbf{x} \sim D} \left[ \frac{1}{2} \mathbf{e}_{\mathcal{P}}^T \mathbb{E}[\mathbf{g}_{\mathcal{P}} \mathbf{g}_{\mathcal{P}}^T] \mathbf{e}_{\mathcal{P}} \right], \quad (13)$$

where a smaller  $s$  indicates that the corresponding atomic expert has less impact on the overall model loss and should be pruned with higher priority. The detailed derivation is provided in Appendix A.

At this point, we have shifted the analysis from the parameter space of atomic experts to their output space, further reducing both computational and storage requirements. Next, we introduce a remarkable property of atomic expert outputs: the outputs of atomic experts within the same expert share identical gradients, *i.e.*,

$$\frac{\partial \ell}{\partial \mathbf{e}^{(i)}(\mathbf{x})} = \frac{\partial \ell}{\partial E(\mathbf{x})}, \quad \forall i \in \{1, \dots, d_{\text{inter}}\}, \mathbf{e}^{(i)} \in E. \quad (14)$$

This property allows us to further significantly reduce storage requirements. Instead of maintaining separate gradient covariance matrices for each atomic expert, we only need to store a single matrix per expert. As a result, the space complexity for computing the importance of the atomic expert within the same expert is drastically reduced to  $\mathcal{O}(d_{\text{model}}^2)$ , enabling efficient storage management.

**Global Ranking of Atomic Experts.** The metric of each atomic expert’s importance has been introduced by equation 13. Next, an important question is how to rank the importance of the atomic experts. Consider that our importance metric evaluates experts based on their overall contribution to the model’s change in the loss function (as shown in equation 2), it provides a natural basis for global ranking. This allows us to effectively compare experts across layers consistently, ensuring that pruning decisions are made based on the entire model’s behavior rather than isolated layer-wise.

270 3.3 HEAPR ALGORITHM  
271

272 Building on the above analysis, we propose HEAPr, a pruning strategy for MoE feedforward layers  
273 that ranks the importance of atomic experts (as defined in equation 13) and removes those with  
274 negligible contribution to the overall loss. To effectively compute the importance of atomic experts,  
275 we leverage a small but representative calibration set  $\mathcal{D}$  and estimate importance in two stages.

276 **1. Shared Gradient Covariance Estimation.** For a given expert  $E_i$ , the gradients of the loss with  
277 respect to all its constituent atomic experts' output are identical. Therefore, rather than performing  
278 redundant computations, we execute a single backward pass to obtain the gradient for the expert's  
279 output,  $\mathbf{g}_{E_i} = \partial \ell / \partial E_i$ . This shared gradient is used to compute a gradient covariance matrix  $\bar{\mathbf{G}}_i$ ,  
280 for all atomic experts belonging to  $E_i$ , accumulated over the subset of tokens  $\mathcal{T}_i \subseteq \mathcal{D}$  routed to  $E_i$ :

$$281 \quad 282 \quad \bar{\mathbf{G}}_i = \frac{1}{|\mathcal{T}_i|} \sum_{\mathbf{x} \in \mathcal{T}_i} \mathbf{g}_{E_i}(\mathbf{x}) \mathbf{g}_{E_i}(\mathbf{x})^\top. \quad (15)$$

283 **2. Importance Computation.** Subsequently, during a forward pass, we compute the importance  
284 for each individual atomic expert  $\mathbf{e}_k$ . Although the gradient covariance matrix  $\bar{\mathbf{G}}_i$  is shared among  
285 all atomic experts within same expert  $E_i$ , the output of each atomic expert,  $\mathbf{e}_k(\mathbf{x})$ , remains unique.  
286 This difference in output allows us to distinguish their individual contributions. The importance of  
287 an atomic expert  $\mathbf{e}_k$  (where  $\mathbf{e}_k \in E_i$ ) is calculated by averaging over the tokens it processes:

$$288 \quad 289 \quad \bar{s}_k = \frac{1}{|\mathcal{T}_i|} \sum_{\mathbf{x} \in \mathcal{T}_i} \frac{1}{2} \mathbf{e}_k(\mathbf{x})^\top \bar{\mathbf{G}}_i \mathbf{e}_k(\mathbf{x}). \quad (16)$$

290 This approach relies solely on standard forward and backward computations, making it both excep-  
291 tionally time- and memory-efficient. The space complexity of each gradient covariance matrix is  
292 only  $\mathcal{O}(d_{\text{model}}^2)$ , significantly alleviating the storage bottleneck. After computing the importance  $\bar{s}_k$   
293 across all micro-experts in the model, we perform a global ranking and prune the lowest  $r\%$  of ex-  
294 perts across all MoE layers. The complete and optimized procedure is summarized in Algorithm 1.

297  
298 **Algorithm 1** HEAPr: Hessian-based Efficient Atomic Expert Pruning

---

299 **Require:** MoE model  $f_\theta$ , calibration set  $\mathcal{D}$ , pruning ratio  $r$   
300 **Ensure:** Pruned model  $f_{\theta'}$

301 1: **for** each expert  $E_i$  **do** ▷ Stage 1: Gradient Covariance Estimation  
302 2:   Collect routed tokens  $\mathcal{T}_i$   
303 3:   Compute shared gradient  $\mathbf{g}_{E_i} = \frac{\partial \ell}{\partial E_i}$   
304 4:   Compute  $\bar{\mathbf{G}}_i = \frac{1}{|\mathcal{T}_i|} \sum_{\mathbf{x} \in \mathcal{T}_i} \mathbf{g}_{E_i}(\mathbf{x}) \mathbf{g}_{E_i}(\mathbf{x})^\top$  ▷ Space complexity  $\mathcal{O}(d^2)$   
305 5: **end for**  
306 6: **for** each atomic expert  $\mathbf{e}_k$  in  $E_i$  **do** ▷ Stage 2: Importance Computation  
307 7:   Compute  $\bar{s}_k = \frac{1}{|\mathcal{T}_i|} \sum_{\mathbf{x} \in \mathcal{T}_i} \frac{1}{2} \mathbf{e}_k(\mathbf{x})^\top \bar{\mathbf{G}}_i \mathbf{e}_k(\mathbf{x})$   
308 8: **end for**  
309 9: Global rank  $\{\bar{s}_k\}$  and prune lowest  $r\%$  across all experts  
310 10: **return** Pruned model  $f_{\theta'}$

---

311  
312313 4 EXPERIMENT  
314315 4.1 EXPERIMENTAL SETUP  
316

317 **Models and Setup.** We evaluate our approach on a broad spectrum of model architectures and  
318 scales to assess its generality and effectiveness, including DeepseekMoE-16B-Base (Dai et al.,  
319 2024), Qwen1.5-MoE-A2.7B-Chat (Team, 2024a), Qwen2-57B-A14B (Team, 2024b), and Qwen3-  
320 30B-A3B. All experiences are calibrated on Wikitext-2 using 128 sequences of 2048 tokens (see  
321 Appendix B for details). Notably, our method introduces no additional tunable hyperparameters.

322 **Baselines.** For our comparisons, we evaluate six recently proposed high-performance compression  
323 methods, including expert dropping (NAEE (Lu et al., 2024), MoE-I<sup>2</sup> (Yang et al., 2024)), expert

324  
 325 Table 1: Performance of HEAPr with DeepSeekMoE-16B-Base, Qwen1.5-MoE-A2.7B-chat,  
 326 Qwen2-57B-A14B and Qwen3-30B-A3B on seven zero-shot tasks, reported in terms of accuracy.  
 327 The results marked with \* are obtained from the official implementation.

328      Ratio	329      Method	Wiki $\downarrow$	PTB $\downarrow$	Openb.	ARC_e	WinoG.	HellaS.	ARC_c	PIQA	MathQA	Avg. $\uparrow$
<b>DeepSeekMoE-16B-Base</b>											
330      0%	Original	6.38	9.47	0.32	0.76	0.71	0.58	0.45	0.79	0.32	0.56
331      20%	NAEE	9.44	15.02	<b>0.32</b>	0.71	0.66	0.55	0.40	0.77	0.29	0.53
	MoE-I <sup>2</sup>	7.69	11.59	0.26	0.71	0.68	0.49	0.38	0.73	0.29	0.50
	MoE-SVD	6.92	10.48	0.31	0.75	0.70	0.53	0.42	0.76	0.31	0.54
	$D^2$ -MoE	6.84	11.10	0.30	0.74	0.69	0.55	0.41	0.76	0.31	0.54
335      40%	<b>HEAPr</b>	<b>6.64</b>	<b>10.51</b>	<b>0.32</b>	<b>0.76</b>	<b>0.71</b>	<b>0.57</b>	<b>0.45</b>	<b>0.79</b>	<b>0.32</b>	<b>0.56</b>
	NAEE	8.55	14.47	0.23	0.67	0.67	0.41	0.32	0.69	0.26	0.46
	MoE-I <sup>2</sup>	9.73	15.75	0.23	0.64	0.66	0.41	0.31	0.68	0.26	0.45
	$D^2$ -MoE	7.93	14.07	0.26	0.69	0.65	0.45	0.36	0.72	0.28	0.49
338	<b>HEAPr</b>	<b>6.91</b>	<b>11.56</b>	<b>0.30</b>	<b>0.74</b>	<b>0.69</b>	<b>0.52</b>	<b>0.41</b>	<b>0.76</b>	<b>0.30</b>	<b>0.53</b>
<b>Qwen1.5-MoE-A2.7B-Chat</b>											
340      0%	Original	8.12	12.97	0.31	0.70	0.66	0.59	0.40	0.79	0.35	0.54
341      25%	MC-SMoE	12.76	17.45	0.25	0.65	0.65	0.53	0.37	-	-	-
	HC-SMoE	11.62	16.39	0.27	0.66	0.63	0.55	0.35	<b>0.76*</b>	0.29*	0.50
	Sub-MoE	9.48	14.84	0.30	<b>0.69</b>	0.66	<b>0.56</b>	0.37	-	-	-
	<b>HEAPr</b>	<b>8.14</b>	<b>14.76</b>	<b>0.32</b>	<b>0.69</b>	<b>0.67</b>	<b>0.56</b>	<b>0.38</b>	<b>0.76</b>	<b>0.35</b>	<b>0.53</b>
344      50%	MC-SMoE	5e2	1e3	0.18	0.33	0.52	0.29	0.19	-	-	-
	HC-SMoE	25.50	38.18	0.23	0.61	<b>0.65</b>	<b>0.47</b>	<b>0.35</b>	0.58*	0.23*	0.45
	Sub-MoE	17.51	29.00	0.25	0.58	0.58	0.46	0.25	-	-	-
	<b>HEAPr</b>	<b>9.23</b>	<b>18.73</b>	<b>0.27</b>	<b>0.64</b>	0.64	0.46	0.33	<b>0.71</b>	<b>0.33</b>	<b>0.48</b>
<b>Qwen3-30B-A3B</b>											
348      0%	Original	8.64	15.40	0.34	0.79	0.71	0.60	0.54	0.79	0.59	0.62
349      25%	HC-SMoE	18.86	31.11	0.22	0.64	0.61	0.40	0.35	0.59*	0.41*	0.46
	Sub-MoE	13.59	23.48	0.25	0.70	0.66	0.47	0.44	-	-	-
	<b>HEAPr</b>	<b>0.33</b>	<b>0.77</b>	<b>0.70</b>	<b>0.55</b>	<b>0.49</b>	<b>0.78</b>	<b>0.50</b>	<b>0.59</b>		
	HC-SMoE	72.33	162.99	0.13	0.44	0.50	0.29	0.23	0.44*	0.32*	0.34
353      50%	Sub-MoE	21.05	43.19	0.23	<b>0.68</b>	0.63	<b>0.41</b>	0.40	-	-	-
	<b>HEAPr</b>	<b>0.25</b>	<b>0.67</b>	<b>0.63</b>	0.38	<b>0.41</b>	<b>0.67</b>	<b>0.36</b>	<b>0.48</b>		
<b>Qwen2-57B-A14B</b>											
355      0%	Original	5.12	9.18	0.33	0.75	0.74	0.63	0.46	0.81	0.39	0.59
356      40%	NAEE	6.81	11.34	0.31	0.73	0.73	0.55	0.46	0.76	0.36	0.55
	MoE-I <sup>2</sup>	24.90	77.05	0.26	0.70	0.46	0.71	0.41	0.75	0.30	0.51
	$D^2$ -MoE	8.19	11.23	<b>0.33</b>	<b>0.75</b>	<b>0.75</b>	0.61	0.45	0.79	0.36	0.58
	<b>HEAPr</b>	<b>5.75</b>	<b>9.59</b>	<b>0.33</b>	<b>0.75</b>	0.74	<b>0.64</b>	<b>0.46</b>	<b>0.81</b>	<b>0.39</b>	<b>0.59</b>

361  
 362 merging (MC-SMoE (Li et al., 2024), HC-SMoE (Chen et al., 2025)), and expert decomposition  
 363 (Sub-MoE (Li et al., 2025a),  $D^2$ -MoE (Gu et al., 2025), MoE-SVD (Li et al., 2025b)). Baseline  
 364 data were collected from prior publications, prioritizing original sources, and details are provided in  
 365 Appendix B. Missing data for open-source implementations were obtained from official code.

366  
 367 **Evaluation.** We report results on seven zero-shot benchmarks using the LM-Evaluation-Harness  
 368 (version 0.4.7) (Gao et al., 2024), including HellaSwag (Zellers et al., 2019), Mathqa (Amini et al.,  
 369 2019), OpenBookQA (OBQA) (Mihaylov et al., 2018), PIQA (Bisk et al., 2020), WinoGrande (Sak-  
 370 aguchi et al., 2021), ARC-Easy and ARC-Challenge (Boratko et al., 2018). These tasks collectively  
 371 enable repeated and consistent evaluation of our method across varied domains and reasoning tasks.

## 372      4.2 MAIN RESULTS

373  
 374 **Compression Performance.** As shown in Table 1, HEAPr achieves exceptional performance  
 375 across various MoE models and compression ratios. Notably, our method delivers near-lossless  
 376 compression. At pruning ratios of 20% ~ 25%, HEAPr matches the performance of the original models  
 377 on DeepSeekMoE-16B-Base and Qwen1.5-MoE-A2.7B-Chat. More impressively, on Qwen2-57B-  
 A14B, HEAPr maintains performance almost identical to the original model even at a high 40%

378 compression ratio. In contrast, our method outperforms recent approaches such as Sub-MoE,  $D^2$ -  
 379 MoE, and NAE $E$  under the same compression ratio. Furthermore, on the latest Qwen3-30B-A3B  
 380 model, HEAPr incurs only a minimal performance loss at a 25% pruning ratio, with the average accu-  
 381 racy dropping slightly from 0.62 to just 0.59. These results strongly highlight the unique advantage  
 382 of HEAPr in pruning at the atomic expert level, enabling substantial model efficiency improvements  
 383 while maintaining and preserving core model performance effectively.

384  
 385 **Compare to CAMERA-P.** In this section, we compare HEAPr with a concurrent related work  
 386 CAMERA-P (Xu et al., 2025), which evaluates the importance of an atomic expert using the  
 387 concept of decoding-time energy. Specifically, the importance of the  $j$ -th atomic expert in the  $i$ -th ex-  
 388 pert is given by  $\varepsilon_{i,j} = (\|\Phi_{i,j}\|_2 + \alpha\|\Phi_{i,j}\|_2) \cdot \|\mathbf{w}_{i,j}^{\text{down}}\|_2$ , where  $\Phi_{i,j} = \text{SiLU}(\mathbf{w}_{i,j}^{\text{gate}} \mathbf{x}) \cdot (\mathbf{w}_{i,j}^{\text{up}} \mathbf{x})$ .  
 389 CAMERA-P uses a heuristic approach to measure atomic expert importance based on the output  
 390 magnitudes on a calibration set. However, this method has two main drawbacks: it is local, neglect-  
 391 ing atomic experts’ impact on overall model performance and cannot be globally applied for pruning  
 392 due to varying activation magnitudes across layers. In contrast, our method HEAPr, built upon the  
 393 OBS framework, leverages the Hessian matrix to assess the impact of atomic experts on the overall  
 394 model performance. And HEAPr yields a globally consistent importance metric for atomic experts,  
 395 thereby enabling principled global pruning, as analyzed in Section 3.2. In Table 2, we compare the  
 396 performance of HEAPr and CAMERA-P on DeepSeekMoE-16B-Base. Since CAMERA-P has not  
 397 released its open-source implementation, we evaluate HEAPr using the `acc_norm` as reported in  
 398 the original paper. At a 20% pruning ratio, HEAPr outperforms CAMERA-P by an average of 1.2  
 399 in accuracy. Even when applying the same layer-wise pruning strategy as CAMERA-P, HEAPr still  
 400 achieves an average accuracy improvement of 0.5. Notably, at a 40% pruning ratio, the performance  
 401 gap between the two methods narrows. We attribute this to the reduced redundancy at higher pruning  
 402 ratio, where the non-essential atomic experts identified by both methods become nearly identical.

403  
 404 **Performance Boundary of Pruning.** Fig-  
 405 ure 2 reports the performance of HEAPr on  
 406 DeepSeekMoE-16B-Base using a random 128-  
 407 sample subset of WikiText-2 with 2048 to-  
 408 kens under different compression ratios, where  
 409 the ratio denotes the fraction of parameters re-  
 410 moved relative to the full model size. For  
 411 compression ratios below 0.4, the pruned mod-  
 412 els retain 0.93% of baseline accuracy while al-  
 413 ready achieving  $0.30\times$  FLOPs savings. In this  
 414 regime, the accuracy curve remains nearly flat,  
 415 revealing substantial redundancy among micro-  
 416 experts and confirming that HEAPr can effec-  
 417 tively identify and remove them. As compres-  
 418 sion increases further, accuracy degrades grace-  
 419 fully, highlighting a clear trade-off between ef-  
 420 ficiency and performance. Even at an extreme  
 421 compression ratio of 0.9%, the model preserves about 38% its baseline accuracy while achieving  
 422  $1.61\times$  FLOP savings. These results demonstrate both the robustness of HEAPr under moderate  
 423 pruning and its effectiveness in enabling aggressive acceleration while retaining performance.

### 4.3 ABLATIONS

424  
 425 **Global vs. Layer-wise Pruning.** As shown in Table 2, layer-wise pruning (Camera-P, HEAPr-L)  
 426 ranks the importance of atomic experts within each MoE layer and prunes the bottom  $r\%$ , whereas  
 427 global pruning (HEAPr-G) ranks the importance of all atomic experts across the entire model. Com-  
 428 pared with Camera-P, our layer-wise pruning HEAPr-L achieves superior performance, indicating  
 429 that the atomic expert importance metric, as derived from equation 13, provides a more effective  
 430 pruning criterion within individual layers. Furthermore, HEAPr-G, by leveraging global pruning  
 431 and importance scores across all layers, achieves even stronger and more consistent results, validat-  
 432 ing the global consistency of the atomic expert importance thoroughly analyzed in Section 3.2.

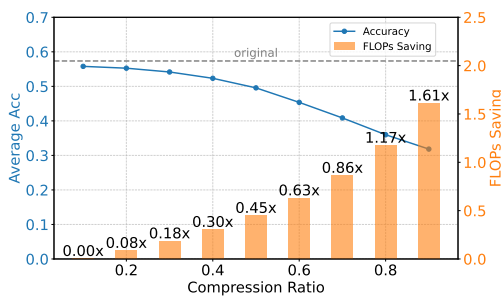


Figure 2: Performance of DeepSeekMoE-16B-Base under varying compression ratios, with corresponding FLOPs saving on WikiText2 data.

432  
 433 Table 2: Comparison of layer-wise pruning (CAMERA-P and HEAPr) versus global pruning  
 434 (HEAPr) on DeepSeekMoE-16B-Base and Qwen1.5-MoE-A2.7B-Chat across seven zero-shot tasks,  
 435 with `acc_norm` reported for DeepSeekMoE-16B-Base and accuracy for others.

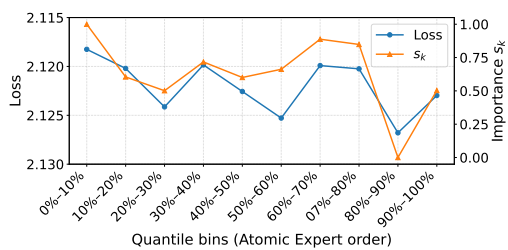
436      Ratio	437      Method	438      Openb.	439      ARC_e	440      WinoG.	441      HellaS.	442      ARC_c	443      PIQA	444      MathQA	445      Average
<b>DeepSeekMoE-16B-Base</b>									
439      20%	CAMERA-P	44.00	71.80	70.17	75.02	45.56	78.62	<b>31.46</b>	59.52
	HEAPr-L	44.01	72.64	70.01	75.55	<b>47.27</b>	79.76	30.92	60.03
	HEAPr-G	<b>44.80</b>	<b>73.73</b>	<b>71.43</b>	<b>76.57</b>	47.01	<b>79.82</b>	31.42	<b>60.68</b>
441      40%	CAMERA-P	<b>43.20</b>	70.71	68.51	69.04	42.24	75.41	29.01	56.87
	HEAPr-L	42.80	70.45	68.35	68.10	43.69	76.12	29.41	56.99
	HEAPr-G	41.40	<b>72.05</b>	<b>69.06</b>	<b>70.79</b>	<b>45.05</b>	<b>76.39</b>	<b>29.85</b>	<b>57.80</b>
<b>Qwen1.5-MoE-A2.7B-Chat</b>									
446      25%	HEAPr-L	30.60	66.58	66.77	55.09	<b>38.05</b>	<b>76.61</b>	33.97	52.52
	HEAPr-G	<b>31.80</b>	<b>68.60</b>	<b>67.22</b>	<b>55.67</b>	37.56	76.39	<b>34.87</b>	<b>53.59</b>
448      50%	HEAPr-L	27.00	63.26	64.01	<b>47.00</b>	33.70	69.80	32.29	48.15
	HEAPr-G	<b>27.01</b>	<b>63.89</b>	<b>64.32</b>	46.35	<b>34.22</b>	<b>70.86</b>	<b>33.37</b>	<b>48.57</b>

450  
 451 **Impact of Pruning Granularity.** To better demonstrate the importance of atomic expert decom-  
 452 position, we conduct an ablation study comparing pruning at the atomic expert level and expert  
 453 level. Based on equation 8, the importance score for an expert computed via equation 13 can be  
 454 expressed as the sum of the importance scores of its constituent atomic experts. As reported in Ta-  
 455 ble 3, expert-level pruning behaves similarly to Expert Dropping (Lu et al., 2024): The activated  
 456 experts unchanged after pruning does not lead to noticeable computational speedup. In contrast,  
 457 pruning at the atomic expert level reduces the dimensionality within each expert, thereby enabling  
 458 real acceleration. Empirically, atomic-level pruning consistently outperforms expert-level pruning  
 459 across multiple benchmarks, highlighting its effectiveness and necessity.

460  
 461 Table 3: Comparison of pruning granularities at the expert level and the atomic expert level, where  
 462 expert importance is computed by summing the importances of its atomic experts, evaluated across  
 463 seven zero-shot tasks. FLOPs rr. denotes the FLOPs reduction ratio.

464      Ratio	465      Level	466      FLOPs rr.↑	467      Wiki↓	468      Openb.	469      ARC_e	470      WinoG.	471      HellaS.	472      ARC_c	473      PIQA	474      MathQA
466      20%	Expert	0%	6.90	31.40	75.76	71.35	<b>57.99</b>	44.31	78.40	30.75
	Atomic Expert	8%	<b>6.64</b>	<b>31.54</b>	<b>75.88</b>	<b>71.43</b>	57.39	<b>44.62</b>	<b>79.05</b>	<b>31.52</b>
468      40%	Expert	0%	8.00	30.60	73.19	63.93	51.15	<b>42.49</b>	<b>77.09</b>	28.24
	Atomic Expert	30%	<b>6.91</b>	<b>30.00</b>	<b>73.78</b>	<b>69.06</b>	<b>52.29</b>	40.61	76.50	<b>30.12</b>

475 **Empirical Correlation of Loss and Atomic**  
 476 **Expert Importance  $s_k$ .** In Section 2, following  
 477 the principles of OBS theory, we define the  
 478 atomic expert importance score  $s_k$  for  $e_p$  based  
 479 on the expected change in model loss. The  
 480 goal of this metric is to identify atomic experts  
 481 whose removal induces the smallest increase in  
 482 the overall loss. However, because both the  
 483 OBS formulation and the output-space approxi-  
 484 mation neglect higher-order terms, an exact nu-  
 485 matical match between  $s_k$  and the empirical  
 486 loss change  $\Delta\ell$  is not expected. Importantly,  
 487 pruning ultimately requires a reliable ranking  
 488 of atomic expert importance rather than an  
 489 accurate prediction of  $\Delta\ell$ . To evaluate the rank-  
 490 ing quality of  $s_k$ , we infer the atomic experts  
 491 on the calibration set and then group them into



492 Figure 3: Consistency between atomic expert normalized  
 493 importance score  $s_k$  and the change in loss. The  
 494 figure plots the actual loss increase  $\Delta\ell$  observed upon  
 495 pruning atomic experts within 10% quantile bins (or-  
 496 dered by original expert index) against the cumulative  
 497 importance  $s_k$ .

486 10% bins according to their original indices. As shown in Table 3, the observed loss increase  $\Delta\ell$  for  
 487 each bin closely follows the cumulative trend of the corresponding normalized importance scores  
 488  $s_k$ . This result indicates that, despite the approximations involved, the proposed  $s_k$  metric provides  
 489 a globally consistent and reliable ranking of atomic experts. It effectively identifies experts whose  
 490 removal causes minimal performance degradation, thereby offering a solid basis for the HEAPr al-  
 491 gorithm and supporting the accuracy of our pruning decisions.

492  
 493 **Impact of Calibration Data.** Table 4 shows  
 494 the average accuracy with error bars over ran-  
 495 dom subsets of the calibration data, indicat-  
 496 ing that the performance of our HEAPr al-  
 497 gorithm is largely unaffected by the choice of  
 498 calibration data, whether they are WikiText-2  
 499 or C4 dataset. This highlights the remarkable  
 500 robustness and generalizability of our method,  
 501 as it consistently performs well across differ-  
 502 ent calibration corpora and domains. Further-  
 503 more, the table also explores the significant im-  
 504 pact of calibration set size on pruning per-  
 505 formance. As the number of calibration samples  
 506 increases, the model’s performance improves  
 507 consistently, indicating that larger calibration  
 508 sets offer richer statistical coverage, which pro-  
 509 vides more reliable and informative signals for effective compression. These results strongly suggest  
 510 that our method is not only robust to variations in calibration data but also benefits from the inclusion  
 511 of additional diverse samples, further enhancing its overall effectiveness and stability.

## 5 CONCLUSION

511  
 512 In this work, we introduce HEAPr, a novel method that refines expert-level pruning in MoE models  
 513 by enabling a more flexible and fine-grained pruning strategy at the atomic expert level. Inspired  
 514 by the principles of the Optimal Brain Surgeon (OBS) theory, we evaluate the importance of atomic  
 515 experts using second-order information. By transforming the analysis from the expert parameter  
 516 space to that of atomic expert parameters, and further shifting it to the atomic expert output space,  
 517 we significantly reduce the computational and storage bottlenecks associated with the second-order  
 518 information matrix. HEAPr requires only two forward passes and one backward pass to efficiently  
 519 compute the importance of atomic experts. Extensive experiments on various modern MoE models  
 520 demonstrate that HEAPr outperforms state-of-the-art pruning methods, achieving near-lossless prun-  
 521 ing with pruning rates of 20%  $\sim$  25%. More importantly, our method provides a much finer-grained  
 522 perspective on MoE expert pruning, which we hope will contribute to a deeper, more comprehen-  
 523 sive understanding of MoE models. Future work will explore large-scale experiments across a wider  
 524 range of model and investigate the potential of parameter compensation methods after the pruning.

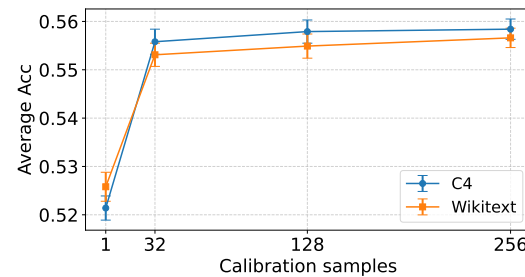
## REFERENCES

525  
 526 Aida Amini, Saadia Gabriel, Peter Lin, Rik Koncel-Kedziorski, Yejin Choi, and Hannaneh Ha-  
 527 jishirzi. Mathqa: Towards interpretable math word problem solving with operation-based for-  
 528 malisms. *arXiv preprint arXiv:1905.13319*, 2019.

529  
 530 Christopher M Bishop and Nasser M Nasrabadi. *Pattern recognition and machine learning*, vol-  
 531 ume 4. Springer, 2006.

532  
 533 Yonatan Bisk, Rowan Zellers, Jianfeng Gao, Yejin Choi, et al. Piqa: Reasoning about physical com-  
 534 monsense in natural language. In *Proceedings of the AAAI conference on artificial intelligence*,  
 535 volume 34, pp. 7432–7439, 2020.

536  
 537 Michael Boratko, Harshit Padigela, Divyendra Mikkilineni, Pritish Yuvraj, Rajarshi Das, Andrew  
 538 McCallum, Maria Chang, Achille Fokoue-Nkoutche, Pavan Kapanipathi, Nicholas Mattei, et al.



539 Figure 4: Performance of DeepSeekMoE-16B-Base  
 540 under a 20% compression ratio, using calibration data  
 541 randomly sampled from WikiText-2 and C4.

540 A systematic classification of knowledge, reasoning, and context within the arc dataset. *arXiv*  
 541 *preprint arXiv:1806.00358*, 2018.  
 542

543 I-Chun Chen, Hsu-Shen Liu, Wei-Fang Sun, Chen-Hao Chao, Yen-Chang Hsu, and Chun-Yi Lee.  
 544 Retraining-free merging of sparse moe via hierarchical clustering. In *Forty-second International*  
 545 *Conference on Machine Learning*, 2025. URL <https://openreview.net/forum?id=hs1OzRxzXL>.  
 546

547 Damai Dai, Chengqi Deng, Chenggang Zhao, RX Xu, Huazuo Gao, Deli Chen, Jiashi Li, Wangding  
 548 Zeng, Xingkai Yu, Yu Wu, et al. Deepseekmoe: Towards ultimate expert specialization in mixture-  
 549 of-experts language models. *arXiv preprint arXiv:2401.06066*, 2024.  
 550

551 Xin Dong, Shangyu Chen, and Sinno Pan. Learning to prune deep neural networks via layer-wise  
 552 optimal brain surgeon. *Advances in neural information processing systems*, 30, 2017.  
 553

554 William Fedus, Barret Zoph, and Noam Shazeer. Switch transformers: Scaling to trillion parameter  
 555 models with simple and efficient sparsity. *Journal of Machine Learning Research*, 23(120):1–39,  
 556 2022.  
 557

558 Elias Frantar and Dan Alistarh. Optimal brain compression: A framework for accurate post-training  
 559 quantization and pruning. *Advances in Neural Information Processing Systems*, 35:4475–4488,  
 560 2022.  
 561

562 Elias Frantar, Saleh Ashkboos, Torsten Hoefler, and Dan Alistarh. OPTQ: Accurate quantization  
 563 for generative pre-trained transformers. In *The Eleventh International Conference on Learning*  
 564 *Representations*, 2023. URL <https://openreview.net/forum?id=tcbBPnfwxs>.  
 565

566 Leo Gao, Jonathan Tow, Baber Abbasi, Stella Biderman, Sid Black, Anthony DiPofi, Charles Fos-  
 567 ter, Laurence Golding, Jeffrey Hsu, Alain Le Noac'h, Haonan Li, Kyle McDonell, Niklas Muen-  
 568 nighoff, Chris Ociepa, Jason Phang, Laria Reynolds, Hailey Schoelkopf, Aviya Skowron, Lin-  
 569 tang Sutawika, Eric Tang, Anish Thite, Ben Wang, Kevin Wang, and Andy Zou. A framework  
 570 for few-shot language model evaluation, 07 2024. URL <https://zenodo.org/records/12608602>.  
 571

572 Hao Gu, Wei Li, Lujun Li, Qiyuan Zhu, Mark Lee, Shengjie Sun, Wei Xue, and Yike Guo. Delta  
 573 decompression for moe-based llms compression. *arXiv preprint arXiv:2502.17298*, 2025.  
 574

575 Babak Hassibi, David G Stork, and Gregory J Wolff. Optimal brain surgeon and general network  
 576 pruning. In *IEEE international conference on neural networks*, pp. 293–299. IEEE, 1993.  
 577

578 Wei Huang, Yue Liao, Jianhui Liu, Ruifei He, Haoru Tan, Shiming Zhang, Hongsheng Li,  
 579 Si Liu, and XIAOJUAN QI. Mixture compressor for mixture-of-experts LLMs gains more. In  
 580 *The Thirteenth International Conference on Learning Representations*, 2025. URL <https://openreview.net/forum?id=hheFYjOsWO>.  
 581

582 Yann LeCun, John Denker, and Sara Solla. Optimal brain damage. *Advances in neural information*  
 583 *processing systems*, 2, 1989.  
 584

585 Lujun Li, Zhu Qiyuan, Jiacheng Wang, Wei Li, Hao Gu, Sirui Han, and Yike Guo. Sub-moe:  
 586 Efficient mixture-of-expert llms compression via subspace expert merging. *arXiv preprint*  
 587 *arXiv:2506.23266*, 2025a.  
 588

589 Pingzhi Li, Zhenyu Zhang, Prateek Yadav, Yi-Lin Sung, Yu Cheng, Mohit Bansal, and Tian-  
 590 long Chen. Merge, then compress: Demystify efficient SMoe with hints from its routing  
 591 policy. In *The Twelfth International Conference on Learning Representations*, 2024. URL  
 592 <https://openreview.net/forum?id=eFWG9Cy3WK>.  
 593

594 Wei Li, Lujun Li, Hao Gu, You-Liang Huang, Mark G. Lee, Shengjie Sun, Wei Xue, and Yike  
 595 Guo. Moe-SVD: Structured mixture-of-experts LLMs compression via singular value decompo-  
 596 sition. In *Forty-second International Conference on Machine Learning*, 2025b. URL <https://openreview.net/forum?id=acJ3vdFljk>.  
 597

594 Wei Li, Lujun Li, You-Liang Huang, Mark G. Lee, Shengjie Sun, Wei Xue, and Yike Guo. Structured  
 595 mixture-of-experts LLMs compression via singular value decomposition, 2025c. URL  
 596 <https://openreview.net/forum?id=ho7ZUS1z8A>.

597

598 Aixin Liu, Bei Feng, Bing Xue, Bingxuan Wang, Bochao Wu, Chengda Lu, Chenggang Zhao,  
 599 Chengqi Deng, Chenyu Zhang, Chong Ruan, et al. Deepseek-v3 technical report. *arXiv preprint*  
 600 *arXiv:2412.19437*, 2024a.

601

602 Enshu Liu, Junyi Zhu, Zinan Lin, Xuefei Ning, Matthew B Blaschko, Shengen Yan, Guohao Dai,  
 603 Huazhong Yang, and Yu Wang. Efficient expert pruning for sparse mixture-of-experts language  
 604 models: Enhancing performance and reducing inference costs. *arXiv preprint arXiv:2407.00945*,  
 605 2024b.

606

607 Xudong Lu, Qi Liu, Yuhui Xu, Aojun Zhou, Siyuan Huang, Bo Zhang, Junchi Yan, and Hongsheng  
 608 Li. Not all experts are equal: Efficient expert pruning and skipping for mixture-of-experts large  
 609 language models. *arXiv preprint arXiv:2402.14800*, 2024.

610

611 James Martens and Roger Grosse. Optimizing neural networks with kronecker-factored approximate  
 612 curvature. In *International conference on machine learning*, pp. 2408–2417. PMLR, 2015.

613

614 Todor Mihaylov, Peter Clark, Tushar Khot, and Ashish Sabharwal. Can a suit of armor conduct  
 615 electricity? a new dataset for open book question answering. *arXiv preprint arXiv:1809.02789*,  
 2018.

616

617 Keisuke Sakaguchi, Ronan Le Bras, Chandra Bhagavatula, and Yejin Choi. Winogrande: An adver-  
 618 sarial winograd schema challenge at scale. *Communications of the ACM*, 2021.

619

620 Sidak Pal Singh and Dan Alistarh. Woodfisher: Efficient second-order approximation for neural  
 621 network compression. *Advances in Neural Information Processing Systems*, 33:18098–18109,  
 2020.

622

623 Qwen Team. Qwen1.5-moe: Matching 7b model performance with 1/3 activated parameters”,  
 624 February 2024a. URL <https://qwenlm.github.io/blog/qwen-moe/>.

625

626 Qwen Team. Qwen2 technical report. *arXiv preprint arXiv:2407.10671*, 2024b.

627

628 Yanyue Xie, Zhi Zhang, Ding Zhou, Cong Xie, Ziang Song, Xin Liu, Yanzhi Wang, Xue Lin, and  
 629 An Xu. Moe-pruner: Pruning mixture-of-experts large language model using the hints from its  
 630 router. *arXiv preprint arXiv:2410.12013*, 2024.

631

632 Yuzhuang Xu, Xu Han, Yuanchi Zhang, Yixuan Wang, Yijun Liu, Shiyu Ji, Qingfu Zhu, and Wanx-  
 633 iang Che. Camera: Multi-matrix joint compression for moe models via micro-expert redundancy  
 634 analysis. *arXiv preprint arXiv:2508.02322*, 2025.

635

636 Cheng Yang, Yang Sui, Jinqi Xiao, Lingyi Huang, Yu Gong, Yuanlin Duan, Wenqi Jia, Miao Yin,  
 637 Yu Cheng, and Bo Yuan. Moe-i2: Compressing mixture of experts models through inter-expert  
 638 pruning and intra-expert low-rank decomposition. In *Findings of the Association for Compu-  
 639 tational Linguistics: EMNLP 2024*, pp. 10456–10466, 2024.

640

641 Shixing Yu, Zhewei Yao, Amir Gholami, Zhen Dong, Sehoon Kim, Michael W Mahoney, and Kurt  
 642 Keutzer. Hessian-aware pruning and optimal neural implant. In *Proceedings of the IEEE/CVF*  
 643 *Winter Conference on Applications of Computer Vision*, pp. 3880–3891, 2022.

644

645 Rowan Zellers, Ari Holtzman, Yonatan Bisk, Ali Farhadi, and Yejin Choi. Hellaswag: Can a ma-  
 646 chine really finish your sentence? *arXiv preprint arXiv:1905.07830*, 2019.

647

648 Qihao Zhu, Daya Guo, Zhihong Shao, Dejian Yang, Peiyi Wang, Runxin Xu, Y Wu, Yukun Li,  
 649 Huazuo Gao, Shirong Ma, et al. Deepseek-coder-v2: Breaking the barrier of closed-source models  
 650 in code intelligence. *arXiv preprint arXiv:2406.11931*, 2024.

648 APPENDIX OVERVIEW  
649

650 • Section A: Derivation of the importance of atomic expert.  
 651 • Section B: Detail Analysis of Main Results.  
 652 • Section C: Analysis of Runtime SpeedUp and Memory Usage.  
 653 • Section D: Compression Rate Analysis under Global Pruning.  
 654 • Section E: Use of LLM.  
 655 • Section F: Reproducibility Statement.  
 656 • Section G: Ethics statement.

659 660 A DERIVATION OF THE IMPORTANCE OF ATOMIC EXPERT  
661

662 We provide a detailed derivation of the importance measure introduced in equation 13.

663 Consider the negative log-likelihood loss  $\ell$ , whose per-sample gradient with respect to the parameters  $\Theta$  can be written as

$$666 \quad \nabla_{\Theta} \ell = \mathbf{J}_k^{\top} \mathbf{g}_{\mathbf{e}_k}, \quad (17)$$

667 where  $\mathbf{J}_k \in \mathbb{R}^{d \times P}$  is the Jacobian of the atomic expert output  $\mathbf{e}_k$  with respect to its parameters  $\Theta$ ,  
 668 and  $\mathbf{g}_{\mathbf{e}_k} \in \mathbb{R}^d$  is the gradient of the loss with respect to  $\mathbf{e}_k$ . By definition, the Fisher Information  
 669 Matrix is

$$671 \quad \bar{\mathbf{H}} = \mathbf{F} = \mathbb{E}[(\nabla_{\Theta} \ell)(\nabla_{\Theta} \ell)^{\top}]. \quad (18)$$

672 After model convergence, the Jacobian  $\mathbf{J}_k$  can be treated as independent (Martens & Grosse, 2015),  
 673 substituting the expression of  $\nabla_{\Theta} \ell$  gives

$$674 \quad \mathbf{F} = \mathbf{J}_k^{\top} \mathbb{E}[\mathbf{g}_{\mathbf{e}_k} \mathbf{g}_{\mathbf{e}_k}^{\top}] \mathbf{J}_k. \quad (19)$$

676 Returning to the quadratic optimization problem in the OBS framework:

$$677 \quad \min_{\delta \Theta} \frac{1}{2} \delta \Theta^{\top} \mathbf{F} \delta \Theta \quad \text{s.t.} \quad \mathbf{J}_k \delta \Theta + \mathbf{e}_k = 0, \quad (20)$$

679 we define the auxiliary variable  $\mathbf{u} = \mathbf{J}_k \delta \Theta$ . The constraint becomes  $\mathbf{u} + \mathbf{e}_k = 0$ , i.e.,  $\mathbf{u} = -\mathbf{e}_k$ ,  
 680 and the objective reduces to

$$682 \quad \min_{\mathbf{u}} \frac{1}{2} \mathbf{u}^{\top} \mathbb{E}[\mathbf{g}_{\mathbf{e}_k} \mathbf{g}_{\mathbf{e}_k}^{\top}] \mathbf{u} \quad \text{s.t.} \quad \mathbf{u} + \mathbf{e}_k = 0. \quad (21)$$

684 Plugging in the constraint yields the optimal cost:

$$685 \quad \Delta \ell = \frac{1}{2} \mathbf{e}_k^{\top} \mathbb{E}[\mathbf{g}_{\mathbf{e}_k} \mathbf{g}_{\mathbf{e}_k}^{\top}] \mathbf{e}_k. \quad (22)$$

687 We therefore define the importance of the  $k$ -th atomic expert as

$$688 \quad s = \frac{1}{2} \mathbf{e}_k^{\top} \mathbb{E}[\mathbf{g}_{\mathbf{e}_k} \mathbf{g}_{\mathbf{e}_k}^{\top}] \mathbf{e}_k \quad (23)$$

690 which is a scalar since  $\mathbf{e}_k \in \mathbb{R}^d$  and  $\mathbb{E}[\mathbf{g}_{\mathbf{e}_k} \mathbf{g}_{\mathbf{e}_k}^{\top}] \in \mathbb{R}^{d \times d}$ . This formalizes equation 13 in the main  
 691 text: the smaller the value of  $s$ , the less impact the  $k$ -th atomic expert has on the overall model loss,  
 692 making it a better candidate for pruning.

693 694 B DETAIL ANALYSIS OF MAIN RESULTS.  
695

696 **Calibration Set Sampling Strategy.** To construct the calibration set, we first load the entire  
 697 dataset (either WikiText-2 or C4) and concatenate all sentences into a single corpus using “\n\n” as  
 698 the separator. We then tokenize the full corpus and split the resulting token stream into consecutive  
 699 samples, each consisting of 2048 tokens. With a fixed random seed (`random.seed(0)`) for repro-  
 700 ducibility, we randomly select 128 such samples to form the calibration set. The 128 samples drawn  
 701 from WikiText were used to obtain all results reported in Table 1, and the impact of the calibration  
 set is discussed in Section 4.3.

702 **Details of Baseline Experiments.** For DeepSeekMoE-16B-Base, the results for NAEE, MoE-I<sup>2</sup>,  
 703 and  $D^2$ -MoE are taken from the paper (Gu et al., 2025), while MoE-SVD results are sourced from  
 704 its paper (Li et al., 2025b). For Qwen1.5-MoE-A2.7B-Chat, all results are from the paper (Li et al.,  
 705 2025a); any missing results with available official open-source code were reproduced by us. For  
 706 Qwen3-30B-A3B, the results for HC-SMoE and Sub-MoE are from the paper (Li et al., 2025a). For  
 707 Qwen2-57B-A14B, the results for NAEE, MoE-I<sup>2</sup>, and  $D^2$ -MoE are taken from the paper (Gu et al.,  
 708 2025). Table ?? shows the calibration dataset size for various methods.

710 Table 4: Calibration set sizes for different methods (2048 sqlen).  
 711

Method	NAEE	$D^2$ -MoE	Sub-MoE	HEAPr
Calibration Set Size	128	512	128	128

715 

## C ANALYSIS OF RUNTIME SPEEDUP AND MEMORY USAGE

719 Table 5 summarizes the computational cost and performance of HEAPr compared with competitive  
 720 baseline methods (NAEE and  $D^2$ -MoE) on two representative MoE models: DeepSeekMoE-16B-  
 721 base and Qwen2-57B-A14B. The table reports the number of calibration samples used for pruning,  
 722 the theoretical FLOPs (TFLOPs) required for pruning, GPU time cost, peak memory usage.

724 Table 5: Comparison of computational cost between HEAPr and baseline pruning methods.  
 725

Method	Samples	TFLOPs	GPU Time Cost	Memory
DeepSeekMoE-16B-base				
NAEE	128	11	2 min	27GB
$D^2$ -MoE	512	227	30 min	53GB
HEAPr	128	44	6 min	44GB
Qwen2-57B-A14B				
NAEE	128	32	8 min	60GB
$D^2$ -MoE	512	1205	90 min	127GB
HEAPr	128	123	20 min	91GB

737 

## D COMPRESSION RATE ANALYSIS UNDER GLOBAL PRUNING

739 In this section, we analyze the compression rates across different layers when applying a 25% and  
 740 50% global pruning strategy based on the global ranking of atomic experts’ importance. As shown  
 741 in Figure 5 and 6, the compression rate is initially high in the early layers, suggesting that the  
 742 experts in these layers are less important and can be pruned with minimal impact on the model’s  
 743 performance. As we move deeper into the network, the compression rate decreases, indicating that  
 744 the experts in these layers are more important to the model’s performance. Interestingly, after a  
 745 certain point, the compression rate starts to increase again in the deepest layers, suggesting that  
 746 some experts in these layers become redundant, allowing for further pruning without significant loss  
 747 of model performance. This non-monotonic behavior highlights the varying importance of experts  
 748 across layers in MoE-based models.

749 

## E USE OF LLMs

752 In this work, Large Language Models (LLMs) were primarily utilized for tasks such as text refine-  
 753 ment, offering writing suggestions, and improving the overall structure and clarity of the manuscript.  
 754 It is important to note that LLMs did not contribute to the ideation or development of the method-  
 755 ology section. The authors guarantee that all LLM-generated content was thoroughly reviewed and  
 756 edited to ensure its accuracy and coherence.

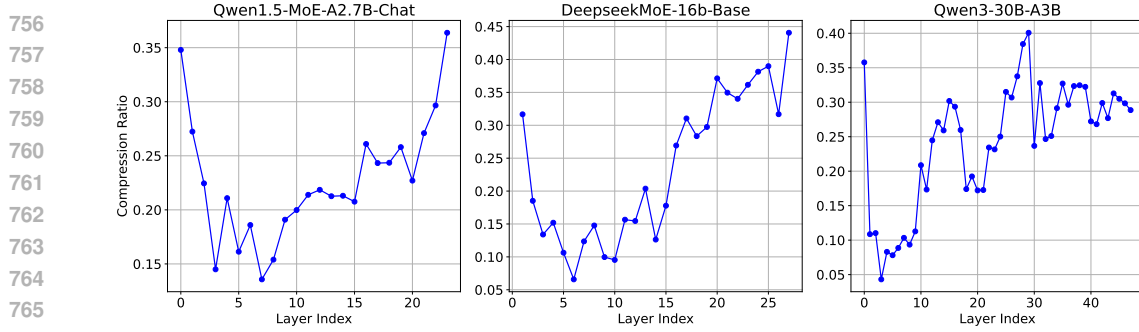


Figure 5: Compression ratios across different layers under 25% global pruning for Qwen1.5-MoE-A2.7B-Chat, DeepSeekMoE-16b-Base, and Qwen3-30B-A3B.

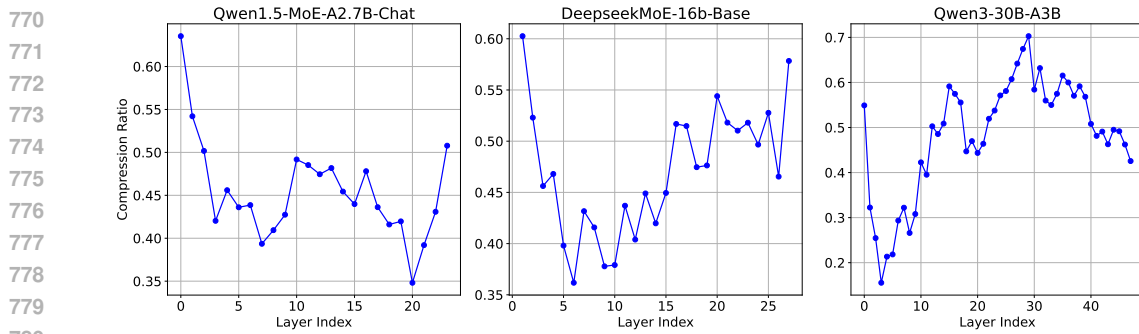


Figure 6: Compression ratios across different layers under 50% global pruning for Qwen1.5-MoE-A2.7B-Chat, DeepSeekMoE-16b-Base, and Qwen3-30B-A3B.

## F REPRODUCIBILITY STATEMENT

To ensure reproducibility, we have made the code and checkpoints obtained in our computational environment available at [anonymous-code-B927](#). While we have taken every effort to ensure consistency, results may exhibit slight variations due to the random selection of calibration sets, as well as potential version differences in libraries such as transformers and LM-Evaluation-Harness. These fluctuations are expected and considered acceptable.

## G ETHICS STATEMENT

This work adheres to ethical guidelines in conducting research and reporting results. We have used publicly available datasets and models, ensuring that our methods comply with their respective terms of use. The research itself aims to enhance existing technologies and does not introduce any ethical concerns. No personal or sensitive data was used in this study, and the methods employed do not raise any known ethical issues.